Inelastic electron tunneling spectroscopy of phenol and hydroquinone chemisorbed on alumina

B. F. Lewis, W. M. Bowser, J. L. Horn Jr., T. Luu, and W. H. Weinberg

Division of Chemistry and Chemical Engineering, and Jet Propulsion Laboratory, California Institute of Technology, Pasadena, California 91103

(Received 13 August 1973)

Inelastic electron tunneling spectroscopy has been used to probe the irreversible chemisorption of C_6H_5OH and 1,4-$C_6H_4(OH)_2$ on a thin amorphous film of Al_2O_3. This spectroscopy yields a representation of the vibronic excitations of the chemical bonds in the adspecies, i.e., the tunneling spectra are analogous to ir spectra. The C_6H_5OH is found to adsorb predominately as $C_6H_5O^-$ with a small amount of adsorption as C_6H_5OH. The 1,4-$C_6H_4(OH)_2$ is found to adsorb predominately as $C_6H_4(OH)O^-$ and perhaps to a smaller extent as $C_6H_4O_2^{2-}$. Extensive hydrogen bonding is observed among adsorbates and between adsorbates and the hydroxylated alumina surface.

INTRODUCTION

The irreversible chemisorption of phenol, C_6H_5OH, and hydroquinone, 1,4-$C_6H_4(OH)_2$, on amorphous alumina has been investigated using inelastic electron tunneling spectroscopy. The inelastic electron tunneling phenomena which will be discussed involve the tunneling of electrons through an insulating oxide barrier between two metal electrodes and the interaction of these electrons with adsorbates at the oxide–metal interface.

In pioneering work, Lambe and Jaklevic[1,2] have shown that the second derivative of the characteristic current–voltage (I–V) function of a tunneling junction is analogous to an ir absorption spectrum. In the case of molecular adsorbates on the insulator surface of tunneling junctions, the molecular symmetry is ordinarily broken so that both Raman and ir vibrational modes are observed. Thus inelastic tunneling spectroscopy is a potentially powerful experimental probe of the chemical interaction of molecules adsorbed on insulating surfaces.

In the present work, inelastic tunneling spectra of phenol and hydroquinone have been measured and compared to Raman and ir spectroscopy for the same adsorbate–adsorbent systems.

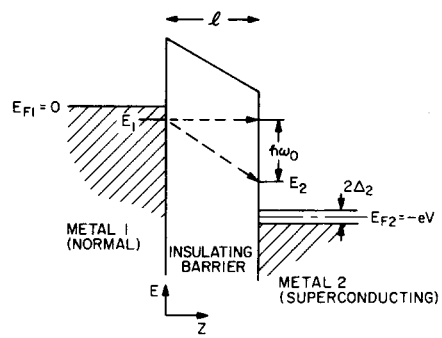

FIG. 1. Schematic diagram for the inelastic electron tunneling between energy level E_1 in a normal metal and energy level E_2 in a superconducting metal of energy gap $2\Delta_2$. The Fermi level of the normal metal is $E_{F1}=0$, while that of the superconducting metal is $E_{F2}=-eV$ where eV is the applied bias voltage. Elastic tunneling is represented by the horizontal dashed line, while inelastic tunneling is represented by the oblique dashed line resulting in a vibronic excitation of energy $\hbar\omega_0$. The width of the insulating barrier is given by l.

THEORY

The theory of inelastic tunneling spectroscopy has been discussed in detail previously[2–5] and will be very briefly reviewed here as it applies to the metal–metal oxide–superconductor junctions used in the present work. Vibronic excitations can occur within the adsorbed molecules present at the oxide insulator surface if $eV \geq \hbar\omega_0 + \Delta_2$, where eV is the bias voltage applied across the vibrational excitation in the adsorbate, and $2\Delta_2$ is the energy gap of the superconductor. The tunneling spectra are measured at temperatures low enough (4.2 K) to insure that all vibrational modes of the adsorbate are in their ground states. An energy diagram describing this physical situation is shown in Fig. 1. Horizontal transitions from energy level E_1 of metal 1 correspond to elastic tunneling, whereas inelastic transitions correspond to an energy loss of $\hbar\omega_0$.

It has been shown that the derivative of the junction conductance, d^2I/dV^2, is analogous to the ir absorption spectrum of the adsorbate.[2] Thus, inelastic electron tunneling spectroscopy may be used to study chemisorption and heterogeneously catalyzed surface reactions in much the same way absorption ir spectroscopy has been employed previously. The d^2I/dV^2 peak intensities are proportional to the surface coverage; and the observed peaks and peak positions reveal which bonds are broken and formed during chemisorption and/or surface reaction. Shifts in peak positions give information about both adsorbate–adsorbent and adsorbate–adsorbate interactions.

EXPERIMENTAL

The tunneling junctions were made by the techniques developed by Lambe and Jaklevic[1,2] and Geiger *et al.*[6] Briefly, this consists of evaporating an Al strip onto a glass slide and then oxidizing the surface of the strip in a glow discharge of pure oxygen. After evacuating the oxygen from the high vacuum system, the oxidized Al_2O_3 strip is exposed to approximately 6 Torr·sec of the desired adsorbate. The adsorbate vapor is then evacuated, and a Pb cross strip is evaporated onto

the oxidized strip. These steps are all conducted in a chamber whose base pressure is on the order of 10^{-6} Torr. Immediately after the junctions are made, they are stored in liquid N_2 and never again warmed up above 77 K. All adsorption experiments are conducted at room temperature.

The tunneling spectra are obtained by measuring the second derivative of the $I-V$ characteristic of the junction. The bias current is modulated with an ultrapure 50-kHz sine wave, and the second harmonic voltage generated across the junction is measured with a lock-in detector. The modulation voltage generated across the sample is usually 2 meV peak-to-peak or less, and the second harmonic voltage is less than 1 μeV rms. During such measurements the samples are immersed in liquid He and can easily be cooled to 1.3 K.

CHEMISORPTION OF PHENOL AND HYDROQUINONE

As described previously, the Al_2O_3 surfaces were given saturation (6-Torr·sec) exposures of both C_6H_5OH and 1,4-$C_6H_4(OH)_2$ at 300 K. The inelastic electron tunneling spectra of the C_6H_5OH and the 1,4-$C_6H_4(OH)_2$ are shown in Figs. 2 and 3, respectively. The various vibronic transitions in both spectra are listed in Tables I and II. Also shown in Table I are the infrared (ir) transitions in vapor, liquid, and solid C_6H_5OH and the Raman transitions of liquid C_6H_5OH.[7,8] The ir transitions of solid and liquid 1,4-$C_6H_4(OH)_2$ and the Raman transitions of liquid 1,4-$C_6H_4(OH)_2$ are shown in Table II.[9] The assignments of the ir and Raman peaks are also given in both Tables I and II.

From the spectrum shown in Fig. 2, it is concluded that most of the C_6H_5OH chemisorbs on Al_2O_3 as a phenoxide ion by cleaving the OH bond in the adsorbate. In tunneling junctions made with no intentionally introduced adsorbate, the oxide surface is saturated with OH groups[2,6,10,11] and the tunneling spectra show OH stretching vibrations (ca. 448 meV) very similar in intensity and shape to those observed for C_6H_5OH junctions. Thus the C_6H_5OH must either displace the "clean" surface OH groups, adsorb with its OH group

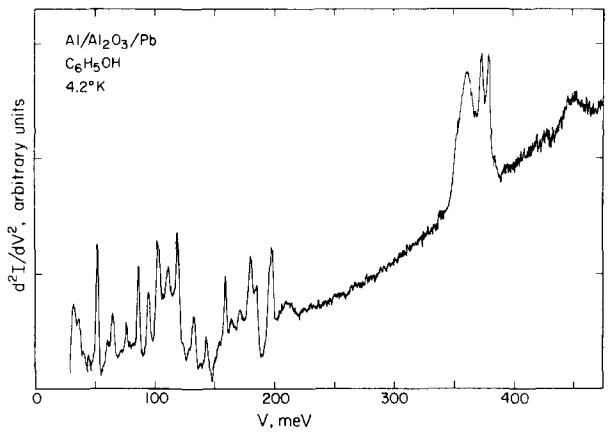

FIG. 2. Inelastic electron tunneling spectrum of C_6H_5OH adsorbed on Al_2O_3 in an $Al/Al_2O_3/Pb$ junction. $T=4.2$ K; junction impedance = 82 Ω; modulation voltage = 2 meV peak-to-peak; oscillator frequency = 46 kHz.

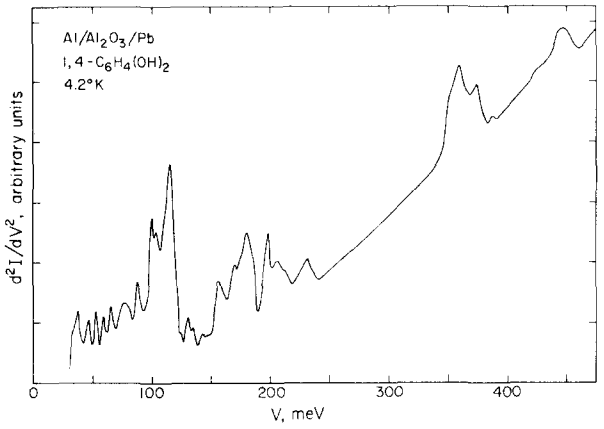

FIG. 3. Inelastic electron tunneling spectrum of 1,4-$C_6H_4(OH)_2$ adsorbed on Al_2O_3 in an $Al/Al_2O_3/Pb$ junction. $T=4.2$ K; junction impedance = 36 Ω; modulation voltage = 2 meV peak-to-peak; oscillator frequency = 47 kHz.

orthogonal to the electric field of the tunneling electrons, or adsorb predominately as a phenoxide ion. In either of the first two cases, the ring stretch with OH-bending-character vibrations at 170.9 and 163.3 meV would be much stronger than is observed. The second case is also unlikely since the oxide is amorphous. There must be a distribution of adsorbate orientations on the surface. Thus most of the C_6H_5OH chemisorbs as a phenoxide ion. However, a small amount of C_6H_5OH evidently chemisorbs on the Al_2O_3 associatively as judged by the weak peaks at 418.8, 170.9, and 163.3 meV. That is, there is a small amount of irreversibly adsorbed molecular C_6H_5OH on the Al_2O_3 after evacuation of the adsorbate from the gas phase at 300 K to a partial pressure $<10^{-5}$ Torr. The strong transition in adsorbed C_6H_5OH present at 118.5 meV is due not only to a CH bending mode of the adsorbate, but also to an Al–O stretching mode in the adsorbent.[2,6,10,11] All of the other transitions are indicative of an adsorbed phenoxide ion chemisorbed to the Al^{3+} site of the Al_2O_3 surface.

It is also clear from Fig. 2 that there is a considerable amount of hydrogen bonding between the adsorbed $C_6H_5O^-$ and presumably adjacent OH groups on the Al_2O_3 surface; this is apparent from the long asymmetric tailing of the OH stretching mode to lower energies. Such a tail is present on the "clean" hydroxylated surface, but is smaller, i.e., there is only a relatively small amount of hydrogen bonding between the OH groups on the otherwise clean Al_2O_3 surface. It should also be noted that Raman modes are evidently active in adsorbed $C_6H_5O^-$ due both to the high intensity of the CH stretching modes and the presence of the 124.4-meV "ring breathing" mode.

The extremely high resolution of IETS is obvious from Fig. 2 and even more apparent when compared with a recent investigation of C_6H_5OH chemisorption on Al_2O_3 using absorption ir spectroscopy.[12] The ir results also indicate that C_6H_5OH is chemisorbed as a phenoxide ion on Al_2O_3 at 425 K, but only five transitions are resolved above 150 meV—CH stretching modes at 378 and 374 meV, aromatic ring vibrations at 199 and 185

TABLE I. Infrared and Raman transitions in phenol and inelastic electron tunneling transitions in phenol adsorbed on an alumina film.[a]

Infrared			Raman	IETS	
Vapor	Liquid	Solid	Liquid	Adsorbate	Assignment
453.9				448.9 (s, b)	
452.9	433.9 (sh)		433.9 (w, b)	418.8 (b)	OH stretch
452.3	415.3 (vs, b)	399.8	415.3 (w)		
381.6	380.6 (w)	380.6 (sh)		382.5 (sh)	
			379.5 (s)	378.1 (s)	
	378.1 (sh)			372.2 (s)	CH stretch
378.1	377.4 (m)	377.3		359.8 (s)	
	374.4 (w)	374.3	374.8	350.6 (sh)	
	198.9 (s)	199.0	199.0 (m)	209.8 (m)	
199.0	198.0 (vs)	198.1	197.8 (m)	197.6 (s)	
186.8					
186.1	186.0 (vs)	186.1	186.0 (w)	184.2 (m)	Ring stretch
185.1					
183.2					
182.3	187.2 (vs)	182.6	182.4 (w)	179.3 (s)	
181.3					
	168.9 (m)	169.9		170.9 (vw)	
167.3					Ring stretch with OH bending character
166.5	166.5 (w)			163.3 (vw)	
165.5					
	160.2 (vvw)	160.2			CH bend
157.2					
156.2		155.2	155.3 (m)	158.4 (s)	X-sensitive
155.3					
	152.2 (vs)	152.5	151.3 (b, w)	154.7 (vw, sh)	
	148.5 (sh)		148.3 (w)		
146.5					OH bending with ring stretch character
145.9					
144.8					
	144.8 (w)	144.9	145.1 (m)	143.1 (m)	
143.6					
142.6	142.8 (w)	142.8	143.2 (m)		
141.6					CH bend
132.9	132.9 (m)	132.9	132.9 (w)	132.7 (m)	
127.9					
127.2	127.1 (w)	127.0	127.0 (m)	127.2 (w)	
126.2					
			124.0 (s)	124.4 (w)	Ring breathing
	121.3 (vvw)	121.6			
		120.8		118.5 (vs)	
	118.8 (vvw)	119.3			(Al–O stretch) CH bend
109.2	110.1 (w)	110.1			
		109.4			
102.0	102.7 (w)	102.7	102.7 (m)	102.7 (s)	
100.9	100.7 (s)	100.7	100.9 (m)		X-sensitive
93.0	93.2 (vs)	93.5	93.6 (w)	94.8 (m)	CH bend
85.1	85.5 (vs)			87.0 (s)	
76.9	76.6 (vw)	76.6	76.5 (m)	76.6 (m)	Ring deformation
66.1					
65.3	65.8	66.3	65.8 (m)	65.3 (m)	
64.2					X-sensitive
62.4	63.0 (m)	62.9	63.1 (w)	60.4 (w)	
		62.2			
	50.8 (b)	51.5	51.5 (b, w)	52.8 (s)	Ring deformation
49.3		56.4		43.5 (w)	X-sensitive

[a] ir and Raman data are taken from Evans (Ref. 7) and Green (Ref. 8). The symbols are defined as follows: b = broad, m = medium, s = strong, sh = shoulder, w = weak, v = very, X = substituent on the aromatic ring.

MeV, and a CO stretching mode (i.e., an x-sensitive mode) at 159 meV.[9] This is in good agreement with the present results, but the much higher resolution of IETS should be emphasized.

The inelastic electron tunneling spectrum of adsorbed 1,4-$C_6H_4(OH)_2$ is shown in Fig. 3, and the results are similar to those of C_6H_5OH. The higher intensity of the 448.1-meV OH stretching mode and its attendant low-energy tail and broad peak at 425.0 meV suggest that one of the OH bonds is preserved in adsorbed 1,4-$C_6H_4(OH)_2$, and the adsorption occurs by cleaving the other OH bond analogous to the mode of adsorption of

TABLE II. Infrared and Raman transitions in hydroquinone and inelastic electron tunneling transitions in hydroquinone adsorbed on an alumina film.[a]

Infrared Solid	Infrared Liquid	Raman Liquid	IETS Adsorbate	Assignment
			448.1 (s, b)	OH stretch
406.4	420.8		425.0 (w, b)	OH stretch
375.7	375.2		388.1 (w)	CH stretch
364.4	367.1		375.6 (m)	CH stretch
363.5	357.3		360.3 (s)	CH stretch
353.6	350.6		352.5 (sh)	CH stretch
337.5	337.5		337.5 (sh)	CH stretch
230.2	230.2		231.9 (w)	Ring stretch
226.9	226.9		207.5 (w)	Ring stretch
201.6	202.1	199.7	197.5 (m)	Ring stretch
187.5	187.5		186.2 (sh)	Ring stretch
181.9	180.4		181.2 (m)	Ring stretch
166.4	165.5		170.0 (sh)	OH bend
161.8	163.3			CH bend
155.0	154.4	156.7	156.8 (m)	OH bend
153.1	152.1	153.2		OH bend
149.2	149.6			OH bend
147.3	148.2			CH bend
144.1	144.1	143.6	143.1 (w)	CH bend
138.4	138.2		135.0 (sh)	CH bend
136.0	136.4		131.2 (m)	CH bend
125.2	125.3		123.8 (sh)	CH bend
116.5	116.2		115.6 (vs)	CH bend
114.1	113.9			CH bend
110.3	111.3			CH bend
102.8	103.2	105.8	105.0 (m)	CH bend
100.4	98.9	102.8	100.8 (m)	CH bend
94.2	94.5		97.2 (sh)	Ring deformation
	93.2		89.0 (m)	CH bend
84.2	83.9		86.0 (sh)	Ring deformation
75.5	75.6	80.7	80.4 (w)	Ring deformation
67.6	67.4		72.0 (w)	Ring deformation
64.3	64.1	65.8	66.8 (w)	Ring deformation
56.9	56.8	58.0	59.8 (m)	Ring deformation
	51.1		53.2 (m)	Ring deformation
	47.7		47.1 (m)	Ring deformation

[a] ir and Raman data taken from Hidalgo and Otero (Ref. 9). Symbols are defined in Table I.

C_6H_5OH (e.g., compare the intensity of the OH stretching to CH stretching modes in 1,4-$C_6H_4(OH)_2$ to those in C_6H_5OH). The possibility of adsorption without cleaving either OH bond cannot be ruled out entirely. Analysis of the data is not yet sufficiently refined to determine whether the OH bending vibrations observed at 170.0 and 156.9 meV are indicative of one or two OH groups per adsorbed molecule. Indeed, there may be di-adsorbed ions (cleaving both OH bonds), especially at low surface coverage. In view of the results for C_6H_5OH, however, it is most probable that adsorption occurs predominately by cleaving one of the OH bonds.

There is a considerable amount of hydrogen bonding apparent for the adsorbed 1,4-$C_6H_4(OH)_2$, even more than in the case of adsorbed C_6H_5OH. This is to be expected in view of the additional OH group present in 1,4-$C_6H_4(OH)_2$. As noted above for the case of C_6H_5OH, the transition at 448.1 and 115.6 meV in Fig. 3 and Table II are indicative to some extent of the Al_2O_3 adsorbent in the absence of any adsorbate.

SUMMARY

Inelastic electron tunneling spectroscopy has been used to probe the chemisorption of phenol and hydroquinone on the surface of an Al_2O_3 film in an Al/Al_2O_3/Pb tunnel junction. The measurement temperature was 4.2 K, and thus the junction was of the type NS with normal Al and superconducting Pb.

Both C_6H_5OH and 1,4-$C_6H_4(OH)_2$ chemisorb irreversibly on the Al^{3+} sites of the Al_2O_3 surface at room temperature. The C_6H_5OH adsorbs predominantly as a $C_6H_5O^-$, and the 1,4-$C_6H_4(OH)_2$ predominantly as a $C_6H_4(OH)O^-$. There is also a small fraction of the Al_2O_3 which chemisorbs associated C_6H_5OH at a room temperature exposure of 6 Torr·sec. The 1,4-$C_6H_4(OH)_2$ may adsorb to a very small extent both in the associated form and also as the di-ion $C_6H_4O_2^{2-}$. There is extensive hydrogen bonding between both the adsorbates, and the adsorbate and the OH groups present on the Al_2O_3 surface as witnessed by the long low-energy tail observed on the OH stretching mode. This occurs for both chemisorbed phenol and hydroquinone to a much greater extent than the hydrogen bonding which exists between the OH groups on the clean, but hydroxylated, Al_2O_3 surface. The high resolution of inelastic electron tunneling spectroscopy is especially evident when compared with adsorption ir data for C_6H_5OH adsorbed on Al_2O_3.[12]

ACKNOWLEDGMENTS

The support of this research by the President's Fund of the California Institute of Technology (Grant No. PF-047) is gratefully acknowledged. We have benefited from the facilities of the Jet Propulsion Laboratory of the California Institute of Technology. JLH and TL wish to thank the Esso Corporation for partial support as participants in the undergraduate research program in the Division of Chemistry and Chemical Engineering at the California Institute of Technology.

[1] R. C. Jaklevic and J. Lambe, Phys. Rev. Lett. **17**, 1139 (1966).
[2] J. Lambe and R. C. Jaklevic, Phys. Rev. **165**, 821 (1968).
[3] D. J. Scalapino and S. M. Marcus, Phys. Rev. Lett. **18**, 459 (1967).
[4] C. B. Duke, *Tunneling in Solids* (Academic, New York, 1969).
[5] *Tunneling Phenomena in Solids*, edited by E. Burstein and S. Lundquist (Plenum, New York, 1969).
[6] A. L. Geiger, B. S. Chandrasekhar, and J. G. Adler, Phys. Rev. **188**, 1130 (1969).
[7] J. C. Evans, Spectrochim. Acta **16**, 1382 (1960).
[8] J. H. S. Green, J. Chem. Soc. **1961**, 2236.
[9] A. Hidalgo and C. Otero, Spectrochim. Acta **16**, 528 (1960).
[10] J. Klein, A. Leger, M. Belin, D. Defourneau, and M. J. L. Sangster, Phys. Rev. **B7**, 2336 (1973).
[11] B. F. Lewis, M. Mosesman, and W. H. Weinberg, Surf. Sci. **41**, 20 (1973).
[12] D. R. Taylor and K. H. Ludlum, J. Phys. Chem. **76**, 2882 (1972).